

# Rapid and accurate detection of novel coronavirus

## SARS-CoV-2 using CRISPR-Cas3

Kazuto Yoshimi<sup>1,2</sup>, Kohei Takeshita<sup>3</sup>, Seiya Yamayoshi<sup>4</sup>, Satomi Shibumura<sup>5</sup>, Yuko Yamauchi<sup>1</sup>, Masaki Yamamoto<sup>3</sup>, Hiroshi Yotsuyanagi<sup>6</sup>, Yoshihiro Kawaoka<sup>4,7</sup>, and Tomoji Mashimo\*<sup>1,2</sup>

<sup>1</sup>*Division of Animal Genetics, Laboratory Animal Research Center, Institute of Medical Science, University of Tokyo, Tokyo 108-8639, Japan,* <sup>2</sup>*Division of Genome Engineering, Center for Experimental Medicine and Systems Biology, Institute of Medical Science, University of Tokyo, Tokyo 108-8639, Japan,* <sup>3</sup>*Life Science Research Infrastructure Group, Advanced Photon Technology Division, RIKEN SPring-8 Center, Hyogo 679-5148 Japan,* <sup>4</sup>*Division of Virology, Department of Microbiology and Immunology, Institute of Medical Science, University of Tokyo, Minato-ku, 108-8639, Tokyo, Japan,* <sup>5</sup>*C4U Corporation, Osaka 565-0871, Japan,* <sup>6</sup>*Division of Infectious Diseases and Applied Immunology, Institute of Medical Science, University of Tokyo, Minato-ku, 108-8639, Tokyo, Japan,* <sup>7</sup>*Department of Pathobiological Sciences, School of Veterinary Medicine, University of Wisconsin-Madison, Madison 53711, Wisconsin, USA*

\*Correspondence to: T.M. ([mashimo@ims.u-tokyo.ac.jp](mailto:mashimo@ims.u-tokyo.ac.jp))

**Novel coronavirus SARS-CoV-2 outbreaks have rapidly spread to multiple countries, highlighting the urgent necessity for fast, sensitive, and specific diagnostic tools for virus surveillance. Here, the previously unknown collateral single-stranded DNA cleavage we observed with type I CRISPR-Cas3 highlights its potential for development as a Cas3-mediated rapid (within 40 min), low-cost, instrument-free detection method for SARS-CoV-2. This Cas3-based assay is comparable with Cas12- and real-time reverse-transcriptase PCR-based assays in its speed and sensitivity, but offers greater specificity for single-base-pair discrimination while negating the need for highly trained operators. These findings support the use of CRISPR diagnostics for point-of-care testing in patients with suspected SARS-CoV-2 infections.**

NOTE: This preprint reports new research that has not been certified by peer review and should not be used to guide clinical practice.

The coronavirus disease 2019 (COVID-19) pandemic caused by the severe acute respiratory syndrome coronavirus 2 (SARS-CoV-2), which emerged in Wuhan, China in late December 2019, has resulted in more than 5.35 million laboratory-confirmed cases in over 210 countries, and more than 340,000 deaths as of May 25, 2020<sup>1,2</sup>. The virus is mainly spread between people during close contact even before the symptoms appear<sup>3</sup>. During the COVID-19 outbreak on the Diamond Princess in Japan in February 2020, 3,700 passengers and crew members were kept aboard the ship for one month, mainly because of the capacity shortage of COVID-19 diagnostic kits<sup>4</sup>. Many countries use assays based on real-time (r) reverse-transcriptase (RT) polymerase chain reaction (PCR) (rRT-PCR) to detect viruses. However, the results of such assays on clinical samples from people with suspected SARS-CoV-2 infections are generally not ready until the day after sample collection because the samples need be shipped to reference laboratories for accurate diagnostic testing<sup>5,6</sup>. rRT-PCR assays also require expensive equipment and well-trained personnel for their operation, making them unsuitable for point-of-care test (POCT) applications, but a POCT would have benefited the situation on the ship.

Enzymes from CRISPR-Cas systems have recently been adapted to rapidly, robustly, and sensitively detect viruses. These systems rely on Cas12a, otherwise called DETECTR (**D**NA **E**ndonuclease-**T**arg**E**ted **C**RISPR **T**rans **R**eporter)<sup>7</sup>, and Cas13, otherwise called SHERLOCK (**S**pecific **H**igh-sensitive **E**nzymatic **R**eporter **U**n**L**O**C**King)<sup>8</sup>. Both of these Cas enzymes, but not Cas9, exhibit nonspecific endonuclease activity in trans after binding to a specific cis target via programmable CRISPR RNAs (crRNAs). By combining isothermal amplification methods (e.g., **R**ecombinase **P**olymerase **A**mplification, RPA<sup>9</sup>; or Loop-mediated isothermal

AMPLification, LAMP<sup>10</sup>) with reporting formats such as lateral flow detection with antigen-labeled reporters<sup>11, 12</sup>, DETECTR<sup>12-14</sup> and SHERLOCK<sup>15, 16</sup> have recently been used for rapid and highly sensitive SARS-CoV-2 detection. The Cas13-based strategy, PAC-MAN (**P**rophylactic **A**ntiviral **C**RISPR in hu**M**AN cells), has also been shown to inhibit and degrade SARS-CoV-2 viral RNA in respiratory epithelial cells<sup>17</sup>.

We and other groups have recently reported that Class 1 Type I-E CRISPR-Cas from *Escherichia coli*<sup>18</sup> and *Thermobifida fusca*<sup>19</sup>, both of which employ a crRNA-bound multiprotein complex (the Cas complex) for antiviral defense (Cascade) and a Cas3 endonuclease, can mediate targeted DNA cleavage with long-range deletions in human cells. Despite type I-E *E. Coli* CRISPR being one of the most thoroughly biochemically characterized *in vitro* plasmid DNA degradation-inducing systems<sup>20, 21</sup>, whether the CRISPR-Cas3 system can mediate the target-activated, nonspecific single-stranded DNA (ssDNA) cleavage reported for Cas12 and Cas13<sup>7, 8</sup> remains an open question. Here, we report on the development of **Cas3-Operated Nucleic Acid detectioN** (CONAN), an *in vitro* nucleic acid-detection platform (Figure 1a). When combined with isothermal amplification methods, CONAN provides a rapid, sensitive and instrument-free detection system for SARS-CoV-2 POCTs.

First, to investigate whether Class 1 CRISPR-Cas3 exhibits trans-cleavage activity on collateral ssDNA, we assembled the *E. Coli* Cas3 protein (20 ng/ $\mu$ L), Cascade with its crRNA (32 ng/ $\mu$ L), the double-stranded DNA (dsDNA) activator (2 ng/ $\mu$ L) for two target genes, human EMX1 or mouse Tyr (Table S1 and S2), and a fluorophore quencher (FQ)-labeled ssDNA probe (4.5 ng/ $\mu$ L) in the reaction buffer (5 mM HEPES-K pH7.5, 60 mM KCl, 10 mM MgCl<sub>2</sub>, 10  $\mu$ M CoCl<sub>2</sub>, and 2.5 mM ATP). After 10 min incubation at 37°C, we observed non-specific trans-ssDNA cleavage after

site-specific dsDNA cutting within the positive (+) strand, but not the negative (-) strand (Figure 1b). We screened all 64 possible target sites containing each of the three-nucleotide protospacer adjacent motif (PAM) sequences (Figure 1c and Fig. S1a), and observed significant cleavage activities with 14 PAM types. The highest activity was from AAG, whereas no activity was seen with the first and the second C nucleotides and the third T nucleotide in the PAM. Therefore, we called this protocol Cas3-Operated Nucleic Acid Detection, or CONAN (Figure 1a).

We then investigated the detection sensitivity of CONAN by diluting the hEMX1 or mTyr dsDNA activator with Cas3, Cascade and FQ-ssDNA in the reaction buffer. CONAN's limit of detection (LoD) was  $>1.0 \times 10^{10}$  copies for the activator (Fig. S1b). To improve the LoD, we performed isothermal RPA at 37°C for 30 min, followed by a 10 min incubation with Cascade and Cas3, thereby determining the activator's single-copy sensitivity level (Figure 1d). We also achieved robust detection of the single-copy activator after mixing it with abundant mouse genomic DNA (Figure 1e).

Detecting FQ-ssDNA cleavage needs a microplate reader for fluorescence intensity measurement. Instead of this laboratory instrument, a lateral flow strip can be used for instrument-free and portable diagnosis by the virus POCT<sup>11, 12</sup>. In principle, abundant reporter accumulates anti-FITC antibody-gold nanoparticle conjugates at the first line (negative) on the strip, while cleavage of the reporter would reduce accumulation on the first line and result in signal on the second line (positive) with  $<2$  min of flow (Fig. S2). Using this lateral flow strip we achieved a one-pot assay with CONAN-RPA, thereby detecting a single copy level of the target dsDNA within 40 min.

We next examined whether the CONAN lateral flow assay would be effective for SARS-CoV-2 diagnosis (Figure 2a), as has been recently reported for

DETECTR<sup>12-14</sup> and for SHERLOCK<sup>15, 16</sup>. We designed primers to amplify the N (nucleoprotein) gene regions (N1 and N2) from SARS-CoV-2 (Table S3), which overlap with the region used in the DETECTOR-based assay<sup>13</sup>, along with primers for the qRT-PCR assay from the US CDC<sup>22</sup>. The qRT-PCR assay successfully amplified both the N1 and N2 regions of SARS-CoV-2, with LoDs of  $<10^2$  copies (Figure 2b). We compared the CONAN- and DETECTR-based assays by designing crRNAs in the N1 and N2 regions (Table S1). However, RT-RPA followed by Cas3-based CONAN or Cas12-based DETECTOR in the one-step 37°C 1-h incubation did not effectively detect SARS-CoV-2, probably because the N1 and N2 primers we designed did not match the sensitivity of the RT-based assay (Fig. S3a).

Designing primers for LAMP assays can be complicated, but the upside is that these assays seem to be less sensitive to inhibitors or off-target nucleic acid contamination in the samples. RT-LAMP at 62°C for 30 min, followed by CONAN or DETECTR for 10 min at 37°C, both specifically detected SARS-CoV-2 with crRNA–N1 and –N2 (Figure 2c). The LoDs for CONAN-LAMP and DETECTR-LAMP ( $<10^2$  copies) compare favorably with the CDC qRT-PCR assay for SARS-CoV-2 detection<sup>5, 13, 23</sup>. This rapid detection by CONAN-LAMP was achieved at 62°C for 30 min, with the lateral flow strip achieving a LoD of  $<10^2$  copies for SARS-CoV-2 (Figure 2d and Supplementary Video).

Finally, we tested the extracted RNA samples from 10 PCR-positive COVID-19 patients and 15 PCR-negative samples from nasopharyngeal swabs, using the CONAN RT-LAMP and DETECTOR RT-LAMP assays with lateral flow strip readouts (Figure 2e). SARS-CoV-2 was detected by the CONAN RT-LAMP assay in 9 of 10 patient swabs and detected in one of 21 negative swab samples (positive predictive

agreement; 90% and negative predictive agreement; 95%). One negative swabs from COVID-19 patients was confirmed to be below the established LoD of  $<10^2$  copies (Fig. S3b). This 94% detection rate (29/31) is comparable with that of the DETECTR RT-LAMP assay in this study (Figure 2e) and that previously reported for a COVID-19 POCT<sup>13</sup>.

CRISPR-based diagnostic (CRISPR-dx) nucleic acid tests have been used to detect the presence DNA or RNA in a range of samples across biotechnology and health areas<sup>7, 8, 24, 25</sup>. They mainly include type V Cas12a DETECTR<sup>12-14</sup> and Cas13 type VI SHERLOCK<sup>15, 16</sup>, which both belong to Class II CRISPR. Here, we report on the discovery of Class I Cas3-mediated collateral trans cleavage activity. Our newly developed a CONAN lateral flow assay, which uses this type of collateral cleavage, facilitated the rapid, robust, and sensitive detection of novel coronavirus SARS-CoV-2. Unlike the single Cas12a and Cas13 platforms, CONAN needs multiple Cas proteins (Cas3, 5, 6, 7, 8, and 11), but they are stable when premixed and stored at around 4°C. Interestingly, unlike DETECTR, CONAN shows high specificity for single-base-pair discrimination within the PAM site (Fig. S4), supporting the applicability of CONAN-based detection assays for POCTs, even with novel emerging coronavirus mutants.

Several other SARS-CoV-2 detection assays and their protocols have been published on the World Health Organization's website or are currently under development<sup>26</sup>. For SARS-CoV-2-based tests, rapid collection of appropriate specimens from patients is a priority goal for clinical management and outbreak control. The RT-PCR-based assays, despite their established efficiency and accuracy for SARS-CoV-2 detection, require highly specialized personnel and expensive equipment

for implementation. In contrast, serology IgM/IgG tests with lateral flow immunoassays can rapidly and sensitively determine the infection rate in a population, although IgG antibodies to SARS-CoV-2 are generally only detectable 10–14 days post-infection. SARS-CoV-2 antigen tests can directly detect viral components without the amplification steps needed for RT-PCR and LAMP; however, the technology is new and the evidence for its accuracy in coronavirus diagnosis is still being evaluated. CRISPR-dx is also cheaper and allows portable diagnostic tests for the assessment of suspected cases without the need for sophisticated equipment. Although still awaiting evaluation, CRISPR-dx methods have high potential for transforming pathogen identification and other aspects of infectious disease diagnostics, such as that relating to SARS-CoV-2.

## **Methods**

### **CRISPR preparation**

CRISPR-Cas3 and CRISPR-Cas12a target sites were based on the human EMX1 gene, the mouse Tyr gene, and the N gene from SARS-CoV-2 (Supplementary Table 1). Cas3 and Cascade proteins from *E. coli* and the crRNA complex (EcoCascade-crRNA) were produced with reference to a previous report, with several modifications<sup>27</sup>. Briefly, the expressed EcoCas3 protein was purified using nickel affinity resin (Ni-NTA, QIAGEN, Venlo, Netherlands) and size-exclusion chromatography (Superdex 200 Increase 10/300 GL; Thermo Fisher Scientific, Waltham, Massachusetts) in 200 mM NaCl, 10% glycerol, 1mM DTT and 20 mM HEPES-Na (pH 7.0). Expressed recombinant Cascade-crRNA was also purified using Ni-NTA resin and size-exclusion

chromatography in 350 mM NaCl, 1mM DTT and 20 mM HEPES-Na (pH 7.0). AsCas12a and LbCas12a were purchased from Integrated DNA Technologies (IDT, Coralville, IA) and New England Biolabs (NEB, Ipswich, Massachusetts), respectively. Target-specific crRNAs were also purchased from IDT.

### **DNA and RNA preparation**

For the CRISPR-Cas3 activator templates, 60 bp fragments of hEMX1 and mTyr (which included a target site) were designed and purchased from IDT. PAM variants in hEMX1 were also designed to examine the correlation between collateral cleavage activity and PAM specificity (Supplementary Table 2). Total mouse genomic DNA from a C57BL/6 strain was used after purification (Maxwell RSC Cell DNA Purification Kit; Promega, Madison, Wisconsin). LAMP SARS-CoV-2 primers were designed against regions of the N gene using PrimerExplorer v.5 (Eiken Chemical Co.; <https://primerexplorer.jp/>). The primers used for isothermal PCR are listed in Supplementary Table 3.

Viral RNAs from SARS-CoV-2 were prepared according to the established protocol from the National Institute of Infectious Diseases in Japan<sup>28</sup>. Viral RNAs were purified from an infected TMPRSS2-expressing VeroE6 cell line using the QIAamp Viral RNA Mini Kit (QIAGEN) according to the manufacturer's protocol. VeroE6/TMPRSS2 cells are available from the Japanese Collection of Research Bioresources Cell Bank in Japan (<https://cellbank.nibiohn.go.jp/english/>) (JCRB no. JCRB1819).

### **Real-time rRT-PCR**

Real-time rRT-PCR was used to determine SARS-CoV-2 RNA copy numbers using

Reliance One-Step Multiplex RT-qPCR Supermix and CFX Connect (Bio-Rad Laboratories, Hercules, CA) according to the manufacturer's protocols. N gene-specific primer and probe sets for real-time rRT-PCR assays and the SARS-CoV-2 plasmid (positive control) were purchased from IDT.

### **CONAN assay**

To characterize the Cas3 collateral cleavage assays, DNA templates were added to 100 nM Cascade-crRNA complex, 250 nM Cas3 and 2.5 mM ATP in CRISPR-Cas3 working buffer (60 mM KCl, 10 mM MgCl<sub>2</sub>, 50 μM CoCl<sub>2</sub>, 5 mM HEPES-KOH pH 7.5), as previously described<sup>27</sup>. The ssDNA reporter probe (5'-5HEX/AAGGTCGGA/ZEN/GTCAACGGATTTGGTC/3IBFQ/-3') (250 nM) was added, and the probe's cleavage-related change in the fluorescence signal was measured every 30 s for 10 min under 37°C incubation.

To detect DNAs, isothermal amplification and RPA were performed using the TwistAmp Basic kit (TwistDx, Maidenhead, UK) according to the manufacturer's protocol. Template DNAs were amplified by incubation at 37°C for 20 min. To detect RNAs, isothermal amplification by the RT-LAMP method was performed using the WarmStart LAMP Kit (NEB) according to the manufacturer's protocol. Template RNAs were reverse transcribed and amplified by incubation at 62 °C for 20 min. To detect low-copy-number molecules in the patients' samples, the incubation time was extended to 30 min.

The CRISPR-Cas3 reaction mixture used for the CONAN method contained 100 nM EcoCascade-crRNA complex, 400 nM Cas3 and 2.5 mM ATP in the working buffer. AsCas12a and LbCas12a were prepared as described previously<sup>13</sup> for use as

positive controls for trans cleavage activity. Cas12a (50 nM) was incubated with 62.5 nM of crRNA in 1× NEBuffer 2.1 for 30 min at 37 °C. After amplification, 2 µl of the amplicon was combined with 18 µl of Cas3 and the Cascade-crRNA complex or the Cas12a-crRNA complex, and 250 nM of the ssDNA reporter probe was added. The fluorescence signal was measured every 30 sec at 37°C.

### **Lateral flow assay**

To optimize the CONAN assay for lateral flow readouts, the CRISPR-Cas3 reaction mixture was added to 200 nM of the Cascade-crRNA complex, with 400 nM Cas3 and 2.5 mM ATP in the working buffer. A 2 µl aliquot of the amplicon was added to 18 µl of Cas3, Cascade-crRNA complex and 500 nM of the ssDNA reporter probe (5'-/5-FITC/TAGCATGTCA/3-Biotin/-3'). The mixture was incubated for 10 min at 37 °C. After adding 50 µl of nuclease-free water, a lateral flow strip (Milenia HybriDetect 1; TwistDx) was added to the reaction tube and the result was visualized after approximately 2 min. A lower band close to the sample pad indicated a negative result (uncut probes), whereas an upper band close to the top of the strip indicated the 5' end of the cut probes. Emergence of an upper band indicated a positive result (Fig. S2).

### **Collection of human clinical samples**

Clinical nasopharyngeal and oropharyngeal swab samples from patients infected with SARS-CoV-2 were collected by IMSUT hospital, according to protocols that were approved by the Research Ethics Review Committee of the Institute of Medical Science, the University of Tokyo. Negative nasopharyngeal swabs were collected from healthy donors at IMSUT. RNA from the samples of patients and healthy donors was extracted

as described in the NIID-approved protocol (input 140  $\mu$ l; elution, 60  $\mu$ l) using the Viral RNA Mini kit (QIAGEN).

## **Data availability**

The data that support the findings of this study are available from the corresponding authors upon reasonable request.

## **Acknowledgments**

We thank Y. Kunihiro, T. Omoto and S. Kobori at Osaka University and M. Hoshi and A. Fukui at Tokyo University and S. Saji, S. Yamamoto, M. Omatsu and N. Godai at the RIKEN SPring-8 Center for their technical assistance. This project was supported in part by JSPS KAKENHI Grant Number 18H03974 (T.M.) and 19K16025 (K.Y.). Partially support also came from the Platform Project for Supporting Drug Discovery and Life Science Research (Basis for Supporting Innovative Drug Discovery and Life Science Research (BINDS)) from AMED under Grant Number JP20am0101070 (support numbers 1251 and 2463), from Research Program on Emerging and Re-emerging Infectious Diseases from AMED (JP19fk0108113), and from the National Institutes of Allergy and Infectious Diseases funded Center for Research on Influenza Pathogenesis (CRIP; HHSN272201400008C). We thank Sandra Cheesman, PhD, from Edanz Group ([www.edanzediting.com/ac](http://www.edanzediting.com/ac)) for editing a draft of this manuscript.

## **Author Contributions**

K.Y. designed and performed most of the experiments and analyzed the data with

assistance from S.S. and Y.Y. K.T. and M.Y. prepared the CRISPR-Cas proteins and performed the experiments. S.Y. H.Y. and Y.K. prepared the clinical samples for CRISPR diagnostic testing. T.M. conceived and supervised the study, prepared the figures and wrote the manuscript with editorial contributions from all the authors.

### **Conflict of interest**

S.S. is employee of C4U. K.Y. and T.M. are co-founders and scientific advisors for C4U. The other authors declare no competing interests.

## References

1. Zhu, N. et al. A Novel Coronavirus from Patients with Pneumonia in China, 2019. *N Engl J Med* **382**, 727-733 (2020).
2. Wang, C., Horby, P.W., Hayden, F.G. & Gao, G.F. A novel coronavirus outbreak of global health concern. *Lancet* **395**, 470-473 (2020).
3. Rothe, C. et al. Transmission of 2019-nCoV Infection from an Asymptomatic Contact in Germany. *N Engl J Med* **382**, 970-971 (2020).
4. Russell, T.W. et al. Estimating the infection and case fatality ratio for coronavirus disease (COVID-19) using age-adjusted data from the outbreak on the Diamond Princess cruise ship, February 2020. *Euro Surveill* **25** (2020).
5. Corman, V.M. et al. Detection of 2019 novel coronavirus (2019-nCoV) by real-time RT-PCR. *Euro Surveill* **25** (2020).
6. Sheridan, C. Coronavirus and the race to distribute reliable diagnostics. *Nat Biotechnol* **38**, 382-384 (2020).
7. Chen, J.S. et al. CRISPR-Cas12a target binding unleashes indiscriminate single-stranded DNase activity. *Science* **360**, 436-439 (2018).
8. Gootenberg, J.S. et al. Nucleic acid detection with CRISPR-Cas13a/C2c2. *Science* **356**, 438-442 (2017).
9. Piepenburg, O., Williams, C.H., Stemple, D.L. & Armes, N.A. DNA detection using recombination proteins. *PLoS Biol* **4**, e204 (2006).
10. Notomi, T. et al. Loop-mediated isothermal amplification of DNA. *Nucleic*

*Acids Res* **28**, E63 (2000).

11. Kellner, M.J., Koob, J.G., Gootenberg, J.S., Abudayyeh, O.O. & Zhang, F. SHERLOCK: nucleic acid detection with CRISPR nucleases. *Nat Protoc* **14**, 2986-3012 (2019).
12. Lucia, C., Federico, P.-B. & Alejandra, G.C. An ultrasensitive, rapid, and portable coronavirus SARS-CoV-2 sequence detection method based on CRISPR-Cas12. *bioRxiv*, 2020.2002.2029.971127 (2020).
13. Broughton, J.P. et al. CRISPR-Cas12-based detection of SARS-CoV-2. *Nat Biotechnol* (2020).
14. Ding, X., Yin, K., Li, Z. & Liu, C. All-in-One Dual CRISPR-Cas12a (AIOD-CRISPR) Assay: A Case for Rapid, Ultrasensitive and Visual Detection of Novel Coronavirus SARS-CoV-2 and HIV virus. *bioRxiv*, 2020.2003.2019.998724 (2020).
15. Ackerman, C.M. et al. Massively multiplexed nucleic acid detection using Cas13. *Nature* (2020).
16. Metsky, H.C., Freije, C.A., Kosoko-Thoroddsen, T.-S.F., Sabeti, P.C. & Myhrvold, C. CRISPR-based surveillance for COVID-19 using genomically-comprehensive machine learning design. *bioRxiv*, 2020.2002.2026.967026 (2020).
17. Abbott, T.R. et al. Development of CRISPR as an Antiviral Strategy to Combat SARS-CoV-2 and Influenza. *Cell* (2020).

18. Morisaka, H. et al. CRISPR-Cas3 induces broad and unidirectional genome editing in human cells. *Nat Commun* **10**, 5302 (2019).
19. Dolan, A.E. et al. Introducing a Spectrum of Long-Range Genomic Deletions in Human Embryonic Stem Cells Using Type I CRISPR-Cas. *Mol Cell* **74**, 936-950 e935 (2019).
20. Hidalgo-Cantabrana, C. & Barrangou, R. Characterization and applications of Type I CRISPR-Cas systems. *Biochem Soc Trans* **48**, 15-23 (2020).
21. Zheng, Y. et al. Endogenous Type I CRISPR-Cas: From Foreign DNA Defense to Prokaryotic Engineering. *Front Bioeng Biotechnol* **8**, 62 (2020).
22. Kimball, A. et al. Asymptomatic and Presymptomatic SARS-CoV-2 Infections in Residents of a Long-Term Care Skilled Nursing Facility - King County, Washington, March 2020. *MMWR Morb Mortal Wkly Rep* **69**, 377-381 (2020).
23. Udugama, B. et al. Diagnosing COVID-19: The Disease and Tools for Detection. *ACS Nano* **14**, 3822-3835 (2020).
24. Petri, K. & Pattanayak, V. SHERLOCK and DETECTR Open a New Frontier in Molecular Diagnostics. *CRISPR J* **1**, 209-211 (2018).
25. Bhattacharyya, R.P., Thakku, S.G. & Hung, D.T. Harnessing CRISPR Effectors for Infectious Disease Diagnostics. *ACS Infect Dis* **4**, 1278-1282 (2018).
26. World Health, O. (World Health Organization, Geneva; 2020).
27. Mulepati, S. & Bailey, S. In vitro reconstitution of an Escherichia coli RNA-guided immune system reveals unidirectional, ATP-dependent degradation

of DNA target. *J Biol Chem* **288**, 22184-22192 (2013).

28. Matsuyama, S. et al. Enhanced isolation of SARS-CoV-2 by TMPRSS2-expressing cells. *Proc Natl Acad Sci U S A* **117**, 7001-7003 (2020).

## Figure Legends

**Figure 1. Cas3-operated nucleic acid detection (CONAN).** **a**, Schematic representation of the CONAN *in vitro* nucleic acid-detection platform. The *E. coli* CRISPR-Cas3 complex contains Cas3, Cas5, Cas6, Cas7, Cas8, and Cas11 proteins and CRISPR RNA (crRNA). FQ-ssDNA, fluorophore and quencher-labeled single-stranded DNA probe. **b**, CRISPR-Cas3 mediates collateral ssDNA cleavage after targeting hEMX1-dsDNA (or mTyr-dsDNA) in fragments with PAMs (+; red), but not in fragments without PAMs (-, black). **c**, Screening for collateral activity on the 64 possible PAM target sites containing each of the three-nucleotide sequences. **d**, CONAN assay on isothermal RPA amplicon products detects a single copy of the activator fragments. **e**, CONAN RPA also detects a single-copy activator when mixed with the abundant mouse genomic DNA. RFU, relative fluorescence unit.

**Figure 2. CRISPR-Cas3-based assay for rapid and sensitive detection of SARS-CoV-2.** **a**, Schematic representation of the CONAN SARS-CoV-2 detection assay including a conventional RNA extraction step, RT-LAMP (62°C, 20–30 min), CONAN (37°C, 10 min), and lateral flow (RT, 2 min). **b**, The limit of detection (LoD) of the US CDC's rRT-PCR assay amplification of the N1 and N2 regions of the SARS-CoV-2 N gene. **c**, LoD of CONAN-based and DETECTR-based assays for the N1 and N2 region of SARS-CoV-2. **d**, LoD of the CONAN-based lateral flow assay for the N1 region of SARS-CoV-2. Cq: cycle quantification value. RFU, relative fluorescence unit. **e**, Comparison of the SARS-CoV-2 CONAN and DETECTR assays using 31 clinical samples (10 positive and 21 negative for COVID-19 by the CDC

rRT-PCR assay). PPA: positive predictive agreement. NPA: negative predictive agreement.

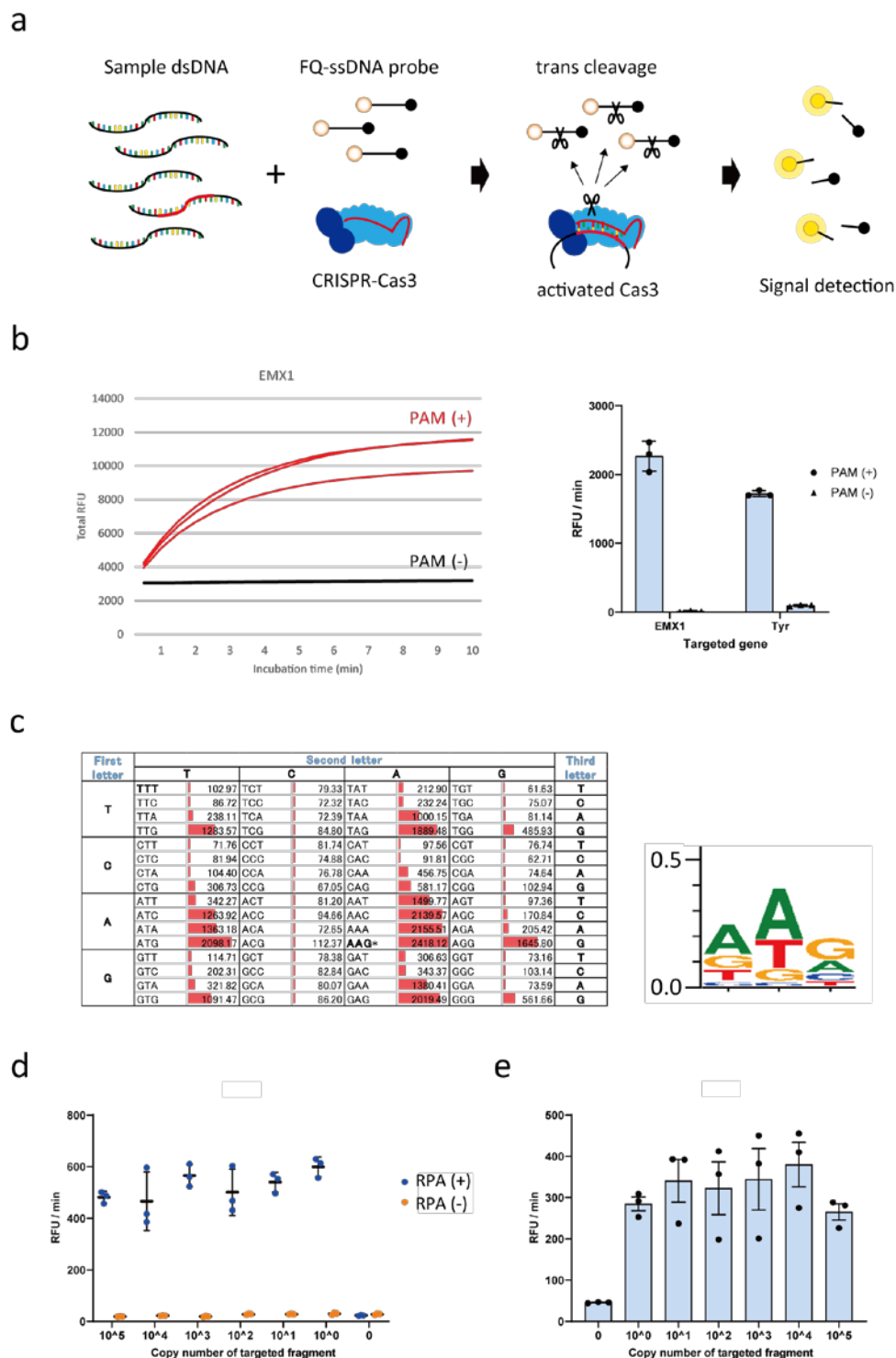
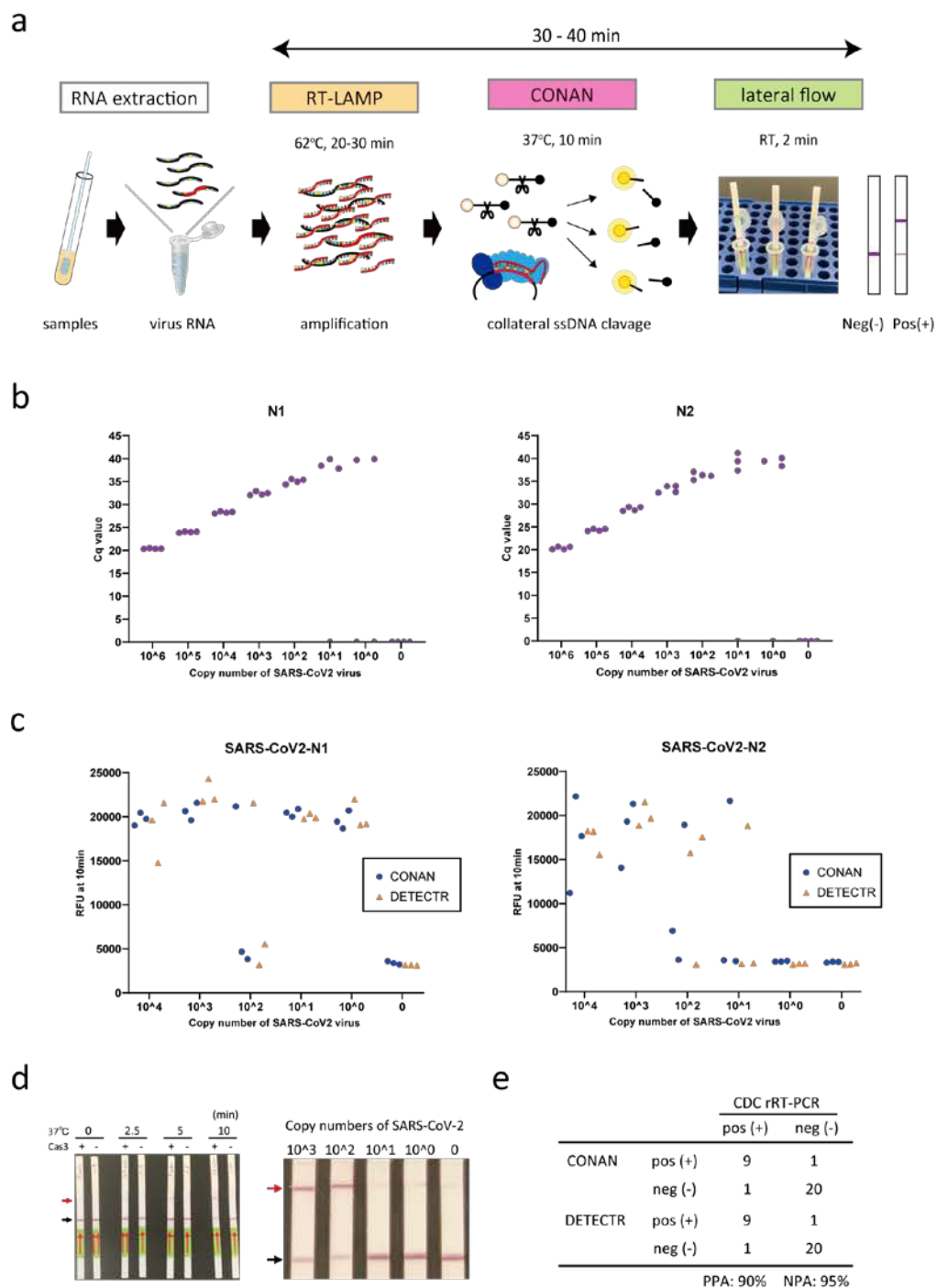


Figure 1



**Figure 2**

# Rapid and accurate detection of novel coronavirus

## SARS-CoV-2 using CRISPR-Cas3

Kazuto Yoshimi<sup>1,2</sup>, Kohei Takeshita<sup>3</sup>, Seiya Yamayoshi<sup>4</sup>, Satomi Shibumura<sup>5</sup>, Yuko Yamauchi<sup>1</sup>, Masaki Yamamoto<sup>3</sup>, Hiroshi Yotsuyanagi<sup>6</sup>, Yoshihiro Kawaoka<sup>4,7</sup>, and Tomoji Mashimo\*<sup>1,2</sup>

<sup>1</sup>*Division of Animal Genetics, Laboratory Animal Research Center, Institute of Medical Science, University of Tokyo, Tokyo 108-8639, Japan,* <sup>2</sup>*Division of Genome Engineering, Center for Experimental Medicine and Systems Biology, Institute of Medical Science, University of Tokyo, Tokyo 108-8639, Japan,* <sup>3</sup>*Advanced Photon Technology Division, RIKEN SPring-8 Center, Hyogo 679-5148 Japan,* <sup>4</sup>*Division of Virology, Department of Microbiology and Immunology, Institute of Medical Science, University of Tokyo, Minato-ku, 108-8639, Tokyo, Japan,* <sup>5</sup>*C4U Corporation, Osaka 565-0871, Japan,* <sup>6</sup>*Division of Infectious Diseases and Applied Immunology, Institute of Medical Science, University of Tokyo, Minato-ku, 108-8639, Tokyo, Japan,* <sup>7</sup>*Department of Pathobiological Sciences, School of Veterinary Medicine, University of Wisconsin-Madison, Madison 53711, Wisconsin, USA*

\*Correspondence to: T.M. ([mashimo@ims.u-tokyo.ac.jp](mailto:mashimo@ims.u-tokyo.ac.jp))

### Supplementary Information

Supplementary Tables 1–3.

Supplementary Figures 1–4.

**Supplementary Table 1. Target sequences for trans cleavage assay.**

Name	PAM (5' to 3')	Sequence (5' to 3')
CRISPR-Cas3		
hEMX1	AAG	CAGGCCAATGGGGAGGACATCGATGTCACCTC
mTyr	AAG	GGACACACTGCTTGGGGGCTCTGAAATATGGA
SARS-N1	ATG	TCTGGTAAAGGCCAACAAACAAGGCCAAAC
SARS-N2	AAG	GAACTGATTACAAACATTGGCCGCAAATTGCA
CRISPR-Cas12a		
hEMX1	TTTG	TGGTTGCCACCCTAGTCATT
SARS-N1	TTTC	TTAGTGACAGTTTGGCCTTG
SARS-N2	TTTG	CCCCAGCGCTTCAGCGTTC

**Supplementary Table 2. DNA fragment sequences for estimating PAM specificity.**

Name	Sequence (5' to 3')
CRISPR-Cas3	
EMX1-AAA-60bp	TGGCGCATTGCCACGAAACAGGCCAATGGGGAGGACATCGATGTCACCTCCAATGACTAG
EMX1-AAC-60bp	TGGCGCATTGCCACGAAACAGGCCAATGGGGAGGACATCGATGTCACCTCCAATGACTAG
EMX1-AAG-60bp	TGGCGCATTGCCACGAAACAGGCCAATGGGGAGGACATCGATGTCACCTCCAATGACTAG
EMX1-AAT-60bp	TGGCGCATTGCCACGAAACAGGCCAATGGGGAGGACATCGATGTCACCTCCAATGACTAG
EMX1-ACA-60bp	TGGCGCATTGCCACGACACAGGCCAATGGGGAGGACATCGATGTCACCTCCAATGACTAG
EMX1-ACC-60bp	TGGCGCATTGCCACGACCCAGGCCAATGGGGAGGACATCGATGTCACCTCCAATGACTAG
EMX1-ACG-60bp	TGGCGCATTGCCACGACGACAGGCCAATGGGGAGGACATCGATGTCACCTCCAATGACTAG
EMX1-ACT-60bp	TGGCGCATTGCCACGACTCAGGCCAATGGGGAGGACATCGATGTCACCTCCAATGACTAG
EMX1-AGA-60bp	TGGCGCATTGCCACGAGACAGGCCAATGGGGAGGACATCGATGTCACCTCCAATGACTAG
EMX1-AGC-60bp	TGGCGCATTGCCACGAGCCAGGCCAATGGGGAGGACATCGATGTCACCTCCAATGACTAG
EMX1-AGG-60bp	TGGCGCATTGCCACGAGGACAGGCCAATGGGGAGGACATCGATGTCACCTCCAATGACTAG
EMX1-AGT-60bp	TGGCGCATTGCCACGATCAGGCCAATGGGGAGGACATCGATGTCACCTCCAATGACTAG
EMX1-ATA-60bp	TGGCGCATTGCCACGATCAGGCCAATGGGGAGGACATCGATGTCACCTCCAATGACTAG
EMX1-ATC-60bp	TGGCGCATTGCCACGATCCAGGCCAATGGGGAGGACATCGATGTCACCTCCAATGACTAG
EMX1-ATG-60bp	TGGCGCATTGCCACGATGACAGGCCAATGGGGAGGACATCGATGTCACCTCCAATGACTAG
EMX1-ATT-60bp	TGGCGCATTGCCACGATTCAGGCCAATGGGGAGGACATCGATGTCACCTCCAATGACTAG
EMX1-CAA-60bp	TGGCGCATTGCCACGCAACAGGCCAATGGGGAGGACATCGATGTCACCTCCAATGACTAG
EMX1-CAC-60bp	TGGCGCATTGCCACGCAACAGGCCAATGGGGAGGACATCGATGTCACCTCCAATGACTAG
EMX1-CAG-60bp	TGGCGCATTGCCACGCAACAGGCCAATGGGGAGGACATCGATGTCACCTCCAATGACTAG
EMX1-CAT-60bp	TGGCGCATTGCCACGCATCAGGCCAATGGGGAGGACATCGATGTCACCTCCAATGACTAG
EMX1-CCA-60bp	TGGCGCATTGCCACGCCACAGGCCAATGGGGAGGACATCGATGTCACCTCCAATGACTAG
EMX1-CCC-60bp	TGGCGCATTGCCACGCCACAGGCCAATGGGGAGGACATCGATGTCACCTCCAATGACTAG
EMX1-CCG-60bp	TGGCGCATTGCCACGCCCAGGCCAATGGGGAGGACATCGATGTCACCTCCAATGACTAG
EMX1-CCT-60bp	TGGCGCATTGCCACGCCCTCAGGCCAATGGGGAGGACATCGATGTCACCTCCAATGACTAG
EMX1-CGA-60bp	TGGCGCATTGCCACGCCGACAGGCCAATGGGGAGGACATCGATGTCACCTCCAATGACTAG
EMX1-CGC-60bp	TGGCGCATTGCCACGCCGACAGGCCAATGGGGAGGACATCGATGTCACCTCCAATGACTAG
EMX1-CGG-60bp	TGGCGCATTGCCACGCCGACAGGCCAATGGGGAGGACATCGATGTCACCTCCAATGACTAG
EMX1-CGT-60bp	TGGCGCATTGCCACGCCGACAGGCCAATGGGGAGGACATCGATGTCACCTCCAATGACTAG
EMX1-CTA-60bp	TGGCGCATTGCCACGCCTCAGGCCAATGGGGAGGACATCGATGTCACCTCCAATGACTAG
EMX1-CTC-60bp	TGGCGCATTGCCACGCCTCAGGCCAATGGGGAGGACATCGATGTCACCTCCAATGACTAG
EMX1-CTG-60bp	TGGCGCATTGCCACGCCTCAGGCCAATGGGGAGGACATCGATGTCACCTCCAATGACTAG
EMX1-CTT-60bp	TGGCGCATTGCCACGCTCAGGCCAATGGGGAGGACATCGATGTCACCTCCAATGACTAG
EMX1-GAA-60bp	TGGCGCATTGCCACGGAACAGGCCAATGGGGAGGACATCGATGTCACCTCCAATGACTAG
EMX1-GAC-60bp	TGGCGCATTGCCACGGACAGGCCAATGGGGAGGACATCGATGTCACCTCCAATGACTAG
EMX1-GAG-60bp	TGGCGCATTGCCACGGACAGGCCAATGGGGAGGACATCGATGTCACCTCCAATGACTAG
EMX1-GAT-60bp	TGGCGCATTGCCACGGATCAGGCCAATGGGGAGGACATCGATGTCACCTCCAATGACTAG
EMX1-GCA-60bp	TGGCGCATTGCCACGGCACAGGCCAATGGGGAGGACATCGATGTCACCTCCAATGACTAG
EMX1-GCC-60bp	TGGCGCATTGCCACGGCCAGGCCAATGGGGAGGACATCGATGTCACCTCCAATGACTAG
EMX1-GCG-60bp	TGGCGCATTGCCACGGCCAGGCCAATGGGGAGGACATCGATGTCACCTCCAATGACTAG
EMX1-GCT-60bp	TGGCGCATTGCCACGGCTCAGGCCAATGGGGAGGACATCGATGTCACCTCCAATGACTAG
EMX1-GGA-60bp	TGGCGCATTGCCACGGGACAGGCCAATGGGGAGGACATCGATGTCACCTCCAATGACTAG
EMX1-GGC-60bp	TGGCGCATTGCCACGGGACAGGCCAATGGGGAGGACATCGATGTCACCTCCAATGACTAG
EMX1-GGG-60bp	TGGCGCATTGCCACGGGACAGGCCAATGGGGAGGACATCGATGTCACCTCCAATGACTAG
EMX1-GGT-60bp	TGGCGCATTGCCACGGGTCAGGCCAATGGGGAGGACATCGATGTCACCTCCAATGACTAG
EMX1-GTA-60bp	TGGCGCATTGCCACGGTACAGGCCAATGGGGAGGACATCGATGTCACCTCCAATGACTAG
EMX1-GTC-60bp	TGGCGCATTGCCACGGTCCAGGCCAATGGGGAGGACATCGATGTCACCTCCAATGACTAG
EMX1-GTG-60bp	TGGCGCATTGCCACGGTCCAGGCCAATGGGGAGGACATCGATGTCACCTCCAATGACTAG
EMX1-GIT-60bp	TGGCGCATTGCCACGGTCCAGGCCAATGGGGAGGACATCGATGTCACCTCCAATGACTAG
EMX1-TAA-60bp	TGGCGCATTGCCACGTAACAGGCCAATGGGGAGGACATCGATGTCACCTCCAATGACTAG
EMX1-TAC-60bp	TGGCGCATTGCCACGTACAGGCCAATGGGGAGGACATCGATGTCACCTCCAATGACTAG
EMX1-TAG-60bp	TGGCGCATTGCCACGTAGCAGGCCAATGGGGAGGACATCGATGTCACCTCCAATGACTAG
EMX1-TAT-60bp	TGGCGCATTGCCACGTATCAGGCCAATGGGGAGGACATCGATGTCACCTCCAATGACTAG
EMX1-TCA-60bp	TGGCGCATTGCCACGTACAGGCCAATGGGGAGGACATCGATGTCACCTCCAATGACTAG
EMX1-TCC-60bp	TGGCGCATTGCCACGTCCAGGCCAATGGGGAGGACATCGATGTCACCTCCAATGACTAG
EMX1-TCG-60bp	TGGCGCATTGCCACGTCCAGGCCAATGGGGAGGACATCGATGTCACCTCCAATGACTAG
EMX1-TCT-60bp	TGGCGCATTGCCACGTCTCAGGCCAATGGGGAGGACATCGATGTCACCTCCAATGACTAG
EMX1-TGA-60bp	TGGCGCATTGCCACGTGACAGGCCAATGGGGAGGACATCGATGTCACCTCCAATGACTAG
EMX1-TGC-60bp	TGGCGCATTGCCACGTGCCAGGCCAATGGGGAGGACATCGATGTCACCTCCAATGACTAG
EMX1-TGG-60bp	TGGCGCATTGCCACGTGCCAGGCCAATGGGGAGGACATCGATGTCACCTCCAATGACTAG
EMX1-TGT-60bp	TGGCGCATTGCCACGTGTCAGGCCAATGGGGAGGACATCGATGTCACCTCCAATGACTAG
EMX1-TTA-60bp	TGGCGCATTGCCACGTTACAGGCCAATGGGGAGGACATCGATGTCACCTCCAATGACTAG
EMX1-TTC-60bp	TGGCGCATTGCCACGTTCCAGGCCAATGGGGAGGACATCGATGTCACCTCCAATGACTAG
EMX1-TTG-60bp	TGGCGCATTGCCACGTTCCAGGCCAATGGGGAGGACATCGATGTCACCTCCAATGACTAG
EMX1-TTT-60bp	TGGCGCATTGCCACGTTTCCAGGCCAATGGGGAGGACATCGATGTCACCTCCAATGACTAG
mTyr-AAG-60bp	GCATTACTATGTGTCAGGGGACACACTGCTTGGGGCTCTGAAATATGGAGGGACATTGA

CRISPR-Cas12a	
EMX1-AAAG-60bp	CAGCACTCTGCCCTCGTGGGAAAGTGGTTGCCACCCCTAGTCATTGGAGGTGACATCGAT
EMX1-AACG-60bp	CAGCACTCTGCCCTCGTGGGAACGTGGTTGCCACCCCTAGTCATTGGAGGTGACATCGAT
EMX1-AAGG-60bp	CAGCACTCTGCCCTCGTGGGAAGGTGGTTGCCACCCCTAGTCATTGGAGGTGACATCGAT
EMX1-AATG-60bp	CAGCACTCTGCCCTCGTGGGAATGTGGTTGCCACCCCTAGTCATTGGAGGTGACATCGAT
EMX1-ACAG-60bp	CAGCACTCTGCCCTCGTGGGACAGTGGTTGCCACCCCTAGTCATTGGAGGTGACATCGAT
EMX1-ACCG-60bp	CAGCACTCTGCCCTCGTGGGACCGTGGTTGCCACCCCTAGTCATTGGAGGTGACATCGAT
EMX1-ACGG-60bp	CAGCACTCTGCCCTCGTGGGACGGTGGTTGCCACCCCTAGTCATTGGAGGTGACATCGAT
EMX1-ACTG-60bp	CAGCACTCTGCCCTCGTGGGACTGTGGTTGCCACCCCTAGTCATTGGAGGTGACATCGAT
EMX1-AGAG-60bp	CAGCACTCTGCCCTCGTGGGAGAGTGGTTGCCACCCCTAGTCATTGGAGGTGACATCGAT
EMX1-AGCG-60bp	CAGCACTCTGCCCTCGTGGGAGCGTGGTTGCCACCCCTAGTCATTGGAGGTGACATCGAT
EMX1-AGGG-60bp	CAGCACTCTGCCCTCGTGGGAGGGTGGTTGCCACCCCTAGTCATTGGAGGTGACATCGAT
EMX1-AGTG-60bp	CAGCACTCTGCCCTCGTGGGAGTGTGGTTGCCACCCCTAGTCATTGGAGGTGACATCGAT
EMX1-ATAG-60bp	CAGCACTCTGCCCTCGTGGGATAGTGGTTGCCACCCCTAGTCATTGGAGGTGACATCGAT
EMX1-ATCG-60bp	CAGCACTCTGCCCTCGTGGGATCGTGGTTGCCACCCCTAGTCATTGGAGGTGACATCGAT
EMX1-ATGG-60bp	CAGCACTCTGCCCTCGTGGGATGGTGGTTGCCACCCCTAGTCATTGGAGGTGACATCGAT
EMX1-ATTG-60bp	CAGCACTCTGCCCTCGTGGGATTGTGGTTGCCACCCCTAGTCATTGGAGGTGACATCGAT
EMX1-CAAG-60bp	CAGCACTCTGCCCTCGTGGGCAAGTGGTTGCCACCCCTAGTCATTGGAGGTGACATCGAT
EMX1-CACG-60bp	CAGCACTCTGCCCTCGTGGGACAGTGGTTGCCACCCCTAGTCATTGGAGGTGACATCGAT
EMX1-CAGG-60bp	CAGCACTCTGCCCTCGTGGGACGGTGGTTGCCACCCCTAGTCATTGGAGGTGACATCGAT
EMX1-CATG-60bp	CAGCACTCTGCCCTCGTGGGACGTGGTTGCCACCCCTAGTCATTGGAGGTGACATCGAT
EMX1-CCAG-60bp	CAGCACTCTGCCCTCGTGGGCCAGTGGTTGCCACCCCTAGTCATTGGAGGTGACATCGAT
EMX1-CCCG-60bp	CAGCACTCTGCCCTCGTGGGCCCGTGGTTGCCACCCCTAGTCATTGGAGGTGACATCGAT
EMX1-CCGG-60bp	CAGCACTCTGCCCTCGTGGGCCGGTGGTTGCCACCCCTAGTCATTGGAGGTGACATCGAT
EMX1-CCTG-60bp	CAGCACTCTGCCCTCGTGGGCCGTGGTTGCCACCCCTAGTCATTGGAGGTGACATCGAT
EMX1-CGAG-60bp	CAGCACTCTGCCCTCGTGGGCGAGTGGTTGCCACCCCTAGTCATTGGAGGTGACATCGAT
EMX1-CGCG-60bp	CAGCACTCTGCCCTCGTGGGCGCGTGGTTGCCACCCCTAGTCATTGGAGGTGACATCGAT
EMX1-CGGG-60bp	CAGCACTCTGCCCTCGTGGGCGGGTGGTTGCCACCCCTAGTCATTGGAGGTGACATCGAT
EMX1-CGTG-60bp	CAGCACTCTGCCCTCGTGGGCGTGGTTGCCACCCCTAGTCATTGGAGGTGACATCGAT
EMX1-CTAG-60bp	CAGCACTCTGCCCTCGTGGGCTAGTGGTTGCCACCCCTAGTCATTGGAGGTGACATCGAT
EMX1-CTCG-60bp	CAGCACTCTGCCCTCGTGGGCTGTGGTTGCCACCCCTAGTCATTGGAGGTGACATCGAT
EMX1-CTGG-60bp	CAGCACTCTGCCCTCGTGGGCTGGTGGTTGCCACCCCTAGTCATTGGAGGTGACATCGAT
EMX1-CTIG-60bp	CAGCACTCTGCCCTCGTGGGCTTGTGGTTGCCACCCCTAGTCATTGGAGGTGACATCGAT
EMX1-GAAG-60bp	CAGCACTCTGCCCTCGTGGGAAAGTGGTTGCCACCCCTAGTCATTGGAGGTGACATCGAT
EMX1-GACG-60bp	CAGCACTCTGCCCTCGTGGGACAGTGGTTGCCACCCCTAGTCATTGGAGGTGACATCGAT
EMX1-GAGG-60bp	CAGCACTCTGCCCTCGTGGGAGGTGGTTGCCACCCCTAGTCATTGGAGGTGACATCGAT
EMX1-GATG-60bp	CAGCACTCTGCCCTCGTGGGATGTGGTTGCCACCCCTAGTCATTGGAGGTGACATCGAT
EMX1-GCAG-60bp	CAGCACTCTGCCCTCGTGGGACAGTGGTTGCCACCCCTAGTCATTGGAGGTGACATCGAT
EMX1-GCCG-60bp	CAGCACTCTGCCCTCGTGGGCCCGTGGTTGCCACCCCTAGTCATTGGAGGTGACATCGAT
EMX1-GCGG-60bp	CAGCACTCTGCCCTCGTGGGCCGGTGGTTGCCACCCCTAGTCATTGGAGGTGACATCGAT
EMX1-GCTG-60bp	CAGCACTCTGCCCTCGTGGGCGTGGTTGCCACCCCTAGTCATTGGAGGTGACATCGAT
EMX1-GGAG-60bp	CAGCACTCTGCCCTCGTGGGAGTGGTTGCCACCCCTAGTCATTGGAGGTGACATCGAT
EMX1-GGCG-60bp	CAGCACTCTGCCCTCGTGGGCGGTGGTTGCCACCCCTAGTCATTGGAGGTGACATCGAT
EMX1-GGGG-60bp	CAGCACTCTGCCCTCGTGGGGGGTGGTTGCCACCCCTAGTCATTGGAGGTGACATCGAT
EMX1-GGTG-60bp	CAGCACTCTGCCCTCGTGGGGTGTGGTTGCCACCCCTAGTCATTGGAGGTGACATCGAT
EMX1-GTAG-60bp	CAGCACTCTGCCCTCGTGGGTAGTGGTTGCCACCCCTAGTCATTGGAGGTGACATCGAT
EMX1-GTCG-60bp	CAGCACTCTGCCCTCGTGGGTCGTGGTTGCCACCCCTAGTCATTGGAGGTGACATCGAT
EMX1-GTGG-60bp	CAGCACTCTGCCCTCGTGGGTGGTGGTTGCCACCCCTAGTCATTGGAGGTGACATCGAT
EMX1-GTTG-60bp	CAGCACTCTGCCCTCGTGGGTTGTGGTTGCCACCCCTAGTCATTGGAGGTGACATCGAT
EMX1-TAAG-60bp	CAGCACTCTGCCCTCGTGGGTAAGTGGTTGCCACCCCTAGTCATTGGAGGTGACATCGAT
EMX1-TACG-60bp	CAGCACTCTGCCCTCGTGGGTACGTGGTTGCCACCCCTAGTCATTGGAGGTGACATCGAT
EMX1-TAGG-60bp	CAGCACTCTGCCCTCGTGGGTAGGTGGTTGCCACCCCTAGTCATTGGAGGTGACATCGAT
EMX1-TATG-60bp	CAGCACTCTGCCCTCGTGGGTATGTGGTTGCCACCCCTAGTCATTGGAGGTGACATCGAT
EMX1-TCAG-60bp	CAGCACTCTGCCCTCGTGGGTACGTGGTTGCCACCCCTAGTCATTGGAGGTGACATCGAT
EMX1-TCCG-60bp	CAGCACTCTGCCCTCGTGGGTCCGTGGTTGCCACCCCTAGTCATTGGAGGTGACATCGAT
EMX1-TCGG-60bp	CAGCACTCTGCCCTCGTGGGTCCGTGGTTGCCACCCCTAGTCATTGGAGGTGACATCGAT
EMX1-TCTG-60bp	CAGCACTCTGCCCTCGTGGGTCTGTGGTTGCCACCCCTAGTCATTGGAGGTGACATCGAT
EMX1-TGAG-60bp	CAGCACTCTGCCCTCGTGGGTGAGTGGTTGCCACCCCTAGTCATTGGAGGTGACATCGAT
EMX1-TGCC-60bp	CAGCACTCTGCCCTCGTGGGTGCGTGGTTGCCACCCCTAGTCATTGGAGGTGACATCGAT
EMX1-TGGG-60bp	CAGCACTCTGCCCTCGTGGGTGGTGGTTGCCACCCCTAGTCATTGGAGGTGACATCGAT
EMX1-TGTG-60bp	CAGCACTCTGCCCTCGTGGGTGTGGTTGCCACCCCTAGTCATTGGAGGTGACATCGAT
EMX1-TTAG-60bp	CAGCACTCTGCCCTCGTGGGTTAGTGGTTGCCACCCCTAGTCATTGGAGGTGACATCGAT
EMX1-TTCG-60bp	CAGCACTCTGCCCTCGTGGGTTCTGTGGTTGCCACCCCTAGTCATTGGAGGTGACATCGAT
EMX1-TTGG-60bp	CAGCACTCTGCCCTCGTGGGTTGGTGGTTGCCACCCCTAGTCATTGGAGGTGACATCGAT
EMX1-TTTG-60bp	CAGCACTCTGCCCTCGTGGGTTTGTGGTTGCCACCCCTAGTCATTGGAGGTGACATCGAT

### Supplementary Table 3. Primer sequences for isothermal PCR

Name	Sequence (5' to 3')
for RPA	
EMX1-F	GAAGAAGGGCTCCCATCACATCAACCGGTG
EMX1-R	GCCAGCAGCAAGCAGCACTCTGCCCTCGTG
SARS-N1-F	CTTGCTTTGCTGCTGCTTGACAGATTGAAC
SARS-N1-R	TTGTTCTGGACCACGTCTGCCGAAAGCTTG
SARS-N2-F	TTCGGCAGACGTGGTCCAGAACAACCCAA
SARS-N2-R	CCTGTGTAGGTCAACCACGTTCCCGAAGGT
for RT-LAMP	
<SARS-N1 set>	
SARS-N1-FIP	GGTTCAATCTGTCAAGCAGCAGTAGAATGGCTGGCAATGG
SARS-N1-BIP	AAGAAGCCTCGGCAAAAACGGTTTGTCTGGACCACGT
SARS-N1-F3	AGTAGGGGAACCTTCTCCTG
SARS-N1-B3	GTCCCCAAAATTCCTTGG
SARS-N1-LF	AGCAAGAGCAGCATCACCG
SARS-N1-LB	CTGCCACTAAAGCATACAATGTAAC
<SARS-N2 set>	
SARS-N2-FIP	TCTGATTAGTTCCTGGTCCCCAAAGCATACAATGTAACACAAGC
SARS-N2-BIP	CGCATTGGCATGGAAGTCACTTTGATGGCACCTGTGTAG
SARS-N2-F3	GCAAAAACGTA CTGCCAC
SARS-N2-B3	GAAATTTGGATCTTTGTCATCC
SARS-N2-LF	TGGACCACGTCTGCCGA
SARS-N2-LB	ACCTTCGGGAACGTGGTT

## Supplementary Figure Legends

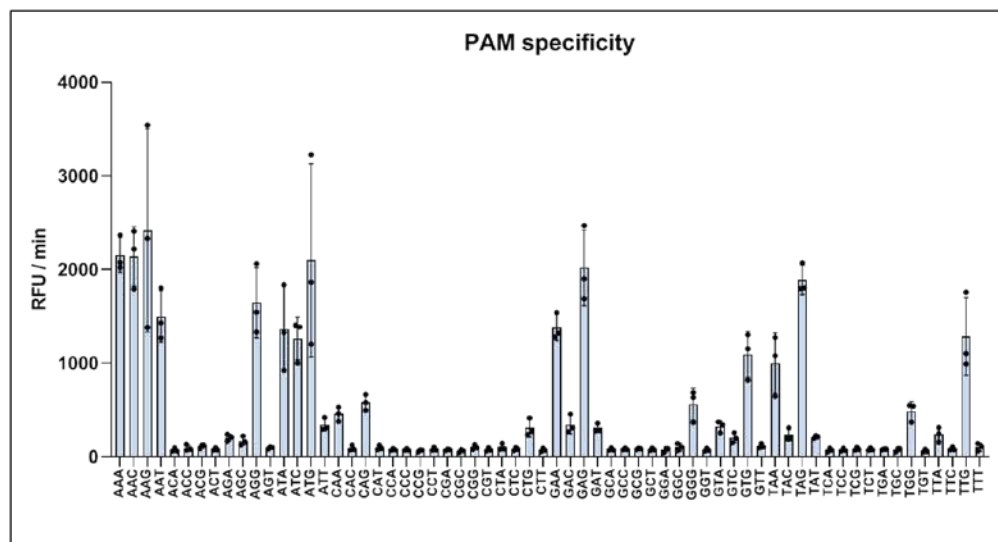
**Supplementary Figure 1. Cas3-operated nucleic acid detection (CONAN).** **a**, CONAN assay screening of the 64 possible PAM target sites containing each of the three-nucleotide sequences (also see **Figure 1c**). **b**, Limit of detection (LoD) of the CONAN assay as estimated by dilution of the dsDNA activators hEMX1 or mTyr with Cas3, Cascade and FQ-ssDNA in the reaction buffer.

**Supplementary Figure 2. Lateral-flow detection with CONAN.** Abundant uncleaved FQ-labeled ssDNA reporter accumulates anti-FITC antibody-gold nanoparticle conjugates on the first line (negative) of the strip, while the cleaved reporter reduces the accumulation at the first line, resulting in a signal on the second line (positive) with a <2 min flow time.

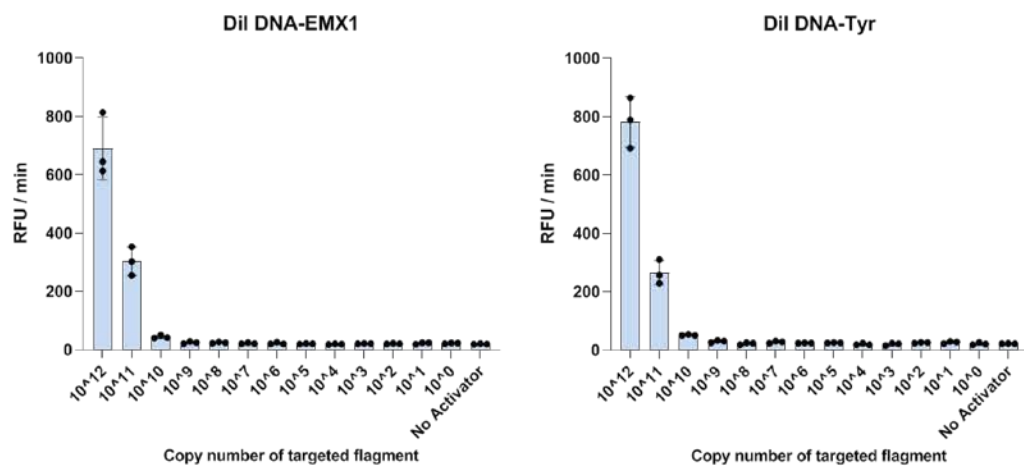
**Supplementary Figure 3.** **a**, Limit of detection of the Cas12a-based DETECTR RT-RPA assay using N1 and N2 primers designed for the N gene region of SARS-CoV-2. **b**, SARS-CoV-2 CONAN lateral flow assays on 10 PCR-positive samples.

**Supplementary Figure 4.** Cas12a-based DETECTR assay screening of the 64 possible target sites containing each of the three-nucleotide PAM sequences.

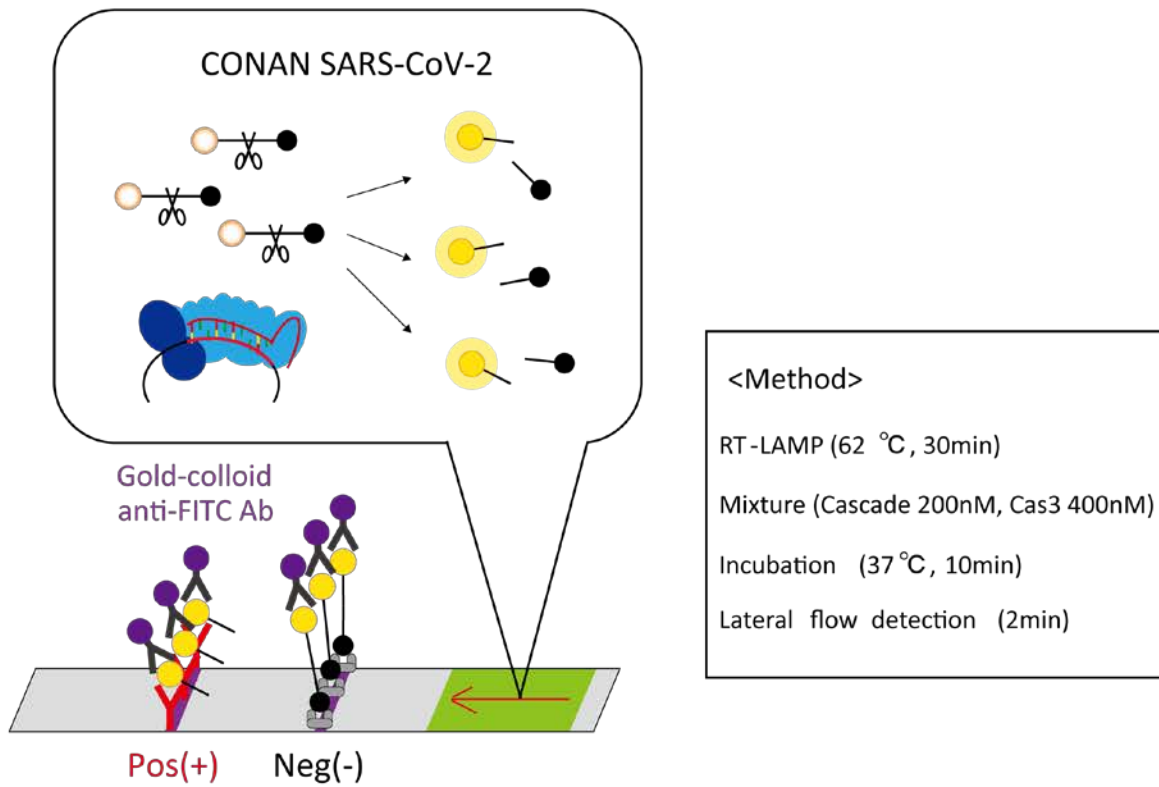
a



b

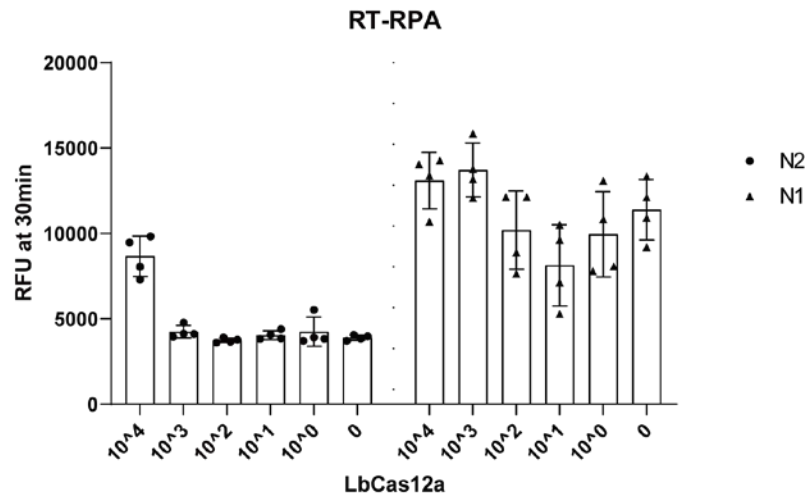


**Supplementary Figure 1**



**Supplementary Figure 2**

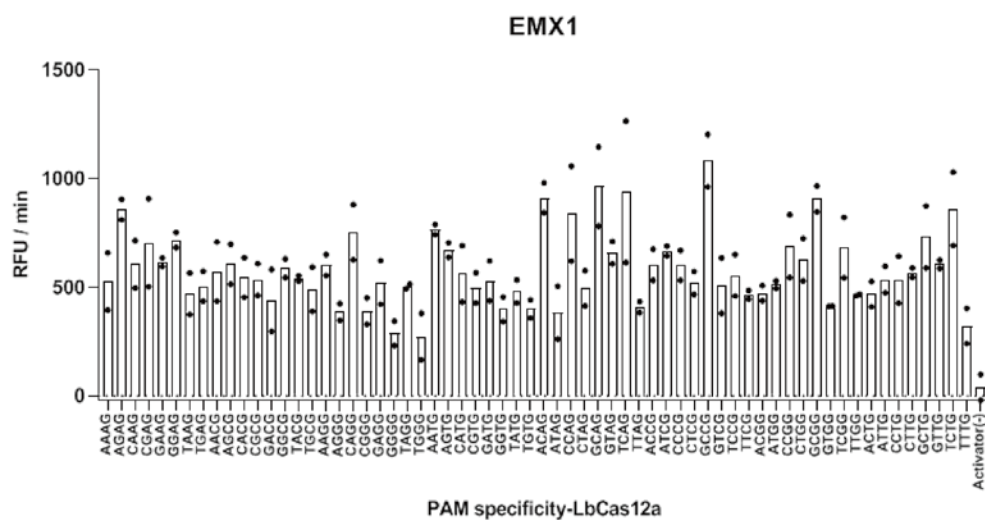
a



b

Sample name	Estimated Copy number from RT-qPCR (/ $\mu$ L)	Image of a lateral flow assay		CONAN detection		Result
		1st	2nd	1st	2nd	
NP- (N1)	-			-	-	Negative Control
NP- (N2)	-			-	-	Negative Control
NPCo-015NT1 (P1)	13688			+	-	Positive (Intermediate)
NPCo-016NT1 (P2)	31522			+	+	Positive
NPCo-018NT1 (P3)	820			-	+	Positive (Intermediate)
NPCo-021NT1 (P4)	12			-	-	Negative
NPCo-021NT2 (P5)	24			+	+	Positive
NPCo-022NT1 (P6)	214			-	+	Positive (Intermediate)
NPCo-023NT1 (P7)	11			+	-	Positive (Intermediate)
NPCo-025NT1 (P8)	797			+	+	Positive
NPCo-025NT2 (P9)	2581			+	+	Positive
NPCo-026NT1 (P10)	7529			+	+	Positive

**Supplementary Figure 3**



First letter	Second letter				Third letter				
	T	C	A	G					
T	TTTG	451.833	TCTG	677.718	TATG	506.291	TGTG	1255.532	T
	TTCG	480.771	TCCG	459.958	TACG	1069.813	TGCG	672.885	C
	TTAG	1195.948	TCAG	791.428	TAAG	342.812	TGAG	440.438	A
	TTGG	782.761	TCGG	809.979	TAGG	882.917	TGGG	376.229	G
C	CTTG	363.813	CCTG	608.364	CATG	560.532	CGTG	757.875	T
	CTCG	466.521	CCCG	450.031	CACG	940.907	CGCG	576.042	C
	CTAG	656.823	CCAG	883.9063	CAAG	669.354	CGAG	742.052	A
	CTGG	528.365	CCGG	781.584	CAGG	1454.729	CGGG	757.761	G
A	ATTG	542.604	ACTG	414.302	AATG	697.906	AGTG	1084.792	T
	ATCG	597.156	ACCG	848.427	AACG	737.125	AGCG	849.323	C
	ATAG	682.281	ACAG	834.406	AAAG*	1574.989	AGAG	822.281	A
	ATGG	677.125	ACGG	399.718	AAGG	970.8542	AGGG	622.375	G
G	GTTG	980.3018	GCTG	784.219	GATG	842.646	GGTG	613.187	T
	GTCG	379.479	GCCG	1262.604	GACG	805.917	GGCG	1014.343	C
	GTAG	901.917	GCAG	777.531	GAAG	1117.656	GGAG	561.969	A
	GTGG	657.417	GCGG	1446.771	GAGG	917.594	GGGG	441.76	G

First	SUM	Second	SUM	Third	SUM
T	11197.31	T	10345.12	T	11141.92
C	11198.66	C	12230.95	C	11611.3
A	12355.66	A	14092.04	A	12995.79
G	13505.31	G	11588.84	G	12507.94

**Supplementary Figure 4**